Separation and Purification Technology 303 (2022) 122199

Contents lists available at ScienceDirect

Separation and Purification Technology

journal homepage: www.elsevier.com/locate/seppur

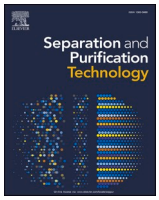

Sequential separation of cobalt and lithium by sorption: Sorbent set selection

N. Conte, J.M. Gómez *, E. Díez, P. Sáez, J.I. Monago, A. Espinosa, A. Rodríguez

Department of Chemical and Materials Engineering (CyPS Research Group), Universidad Complutense de Madrid, 28040 Madrid, Spain

ARTICLE INFO

Keywords:
Cobalt
Lithium
Selective sorption
Sorbents
Solid buffer

ABSTRACT

The sorption of cobalt and lithium was studied using low-cost natural (dolomite, diatomite, barite), commercial (13X zeolites and clinoptilolite) and synthesized (mesoporous carbon and NaY zeolite) sorbents. The pH of the medium was a key factor in the sorption process which can be modified due to the active chemical groups on the surface of the sorbents. Therefore, the doses of each sorbent were selected to avoid cobalt precipitation, working at pH below 8. Sorption with monometallic solution was carried out to select the best set of sorbents for subsequent selective separation. Only mesoporous activated carbon and dolomite allow to achieve significant cobalt removal, 85% and 65% respectively, with negligible lithium removal. 13X zeolite (high surface area and low Si/Al molar ratio) removed both metals without selectivity. Therefore, dolomite and mesoporous activated carbon were selected for the selective separation of cobalt, as they allow to achieve an adsorbed Co^{2+}/Li^{+} weight ratio of 16 and 4, respectively. 13X was selected to remove lithium once cobalt was removed from the solution. The best separation was carried out by a two-sequential sorption stage, using dolomite in a first stage to separate cobalt and 13X zeolite in a second stage to remove lithium, reaching an almost complete removal of both metals. The pH control for working with high doses of dolomite was achieved by means of a solid phase pH buffer (solid buffer) composed by a mixture of the dolomite itself and non-activated mesoporous carbon (without sorption capacity) in a 1:4 weight ratio. This solid buffer allowed the pH of the medium to be controlled to around 6.5.

1. Introduction

Water plays an essential role within the sustainable development concept, not only for being an essential good for life, but also for its relevance in the energy production [1]. Population growth involves in parallel a rise in the demand of water, energy and food, which is completely unsustainable in the long term [2]. As a consequence, water pollution has emerged as one of the most important environmental issues that humanity must face in the present century, to ensure the sustainable development of the society, covering the requirements for the present and future generations [3]. Human activity appears to be the main reason for the pollutant emissions to water. The potential hazard and the corresponding treatment for each pollutant will depend on their nature [4]. Particularly hazardous is the heavy metal pollution in water. Their danger for human organism and environment lies in their bioaccumulation and their biomagnification towards lower levers through the trophic chain [5]. Heavy metal emissions commonly have an anthropogenic origin, with punctual sources like metallurgic, chemical, electronic and mining industries [6]. There are also uncontrolled discharges that can cause these metals to reach water springs. Among heavy metals, some of them, due to their low levels of production and recycling rate, their economic importance, risk of supply or unique features, are known as critical raw materials [7]. Therefore, their recycling and reuse will be crucial for the sustainable development [8], and can contribute to achieving the sixth (clean water and sanitation) and seventh (affordable and clean energy) goals of the Sustainable Development Goals (SDGs) [9].

Cobalt and lithium are two of the most important strategic metals, due to their properties for the manufacture of ion-lithium batteries for electric vehicles [10], electronic devices and energy storage [11]. Both metals coexist in spent lithium-ion batteries (LiB) being part of the cathode solution and must be separated during their recovery in the recycling process. Their demand in the UE for 2050 [7] is forecasted to be up to 15 times higher for cobalt and even 60 times higher for lithium, regarding to the actual required levels [12]. The massive consumption of those devices, together with the generally irresponsible attitude of the users, can generate huge amounts of waste. Those wastes can end up in electronic scrap landfills and aqueous streams, occasioning Co and Li

* Corresponding author.
E-mail address: segojmgm@ucm.es (J.M. Gómez).

https://doi.org/10.1016/j.seppur.2022.122199
Received 12 July 2022; Received in revised form 8 September 2022; Accepted 20 September 2022
Available online 24 September 2022

leaching issues [13]. Those aqueous waste flows have the potential to be exploited to recover the cobalt and lithium, for their further reuse [10]. Thus, both recovery of these strategic metals and the wastewater treatment is desired, approaching the circular economy concept [12], preserving the natural resources and minimizing the environmental impact. Although it has been a relevant topic in the past, in years to come research in battery metals is expected to witness a considerable rise, since low-carbon economy needs to be achieved and electric vehicles seem to be one of the vectors of the change [7].

There is a wide range of technologies that allow the heavy metal removal from wastewater. Chemical precipitation, membrane filtration, ion exchange, adsorption and electrochemical treatments are commonly used [14]. Among these methods, adsorption arises as a reliable alternative for the removal of metals from wastewater. Adsorption is recognized as being one of the most popular methods due to its advantages, which include: low cost, ease of operation and implementation, high efficiency, and the possibility of using adsorbent materials from a wide range of origins. This operation is especially adequate when the metal to be separated is presented at low concentrations [15]. Additionally, it can be used as a technology for the preconcentration of heavy metals in the wastewater flows, so that they can be recovered or treated with other treatments [16] like hydrometallurgy [17], pyrometallurgy [18], solvent extraction [19] and Donnan dialysis processes [20]. Not only that, but adsorption can be integrated in a tertiary treatment of a wastewater treatment plant, as a complement in order to adsorb those compounds not removed in the biological treatment [21]. In the recycling process of battery metals, adsorption can be incorporated as a final stage in the removal of these metals (cobalt, lithium, nickel, etc.) [22]. Besides, it would be right to treat the outlet stream after leaching solution treatment by hydrometallurgical or pyrometallurgical processes [23], liquid–liquid extraction, precipitation, etc. that allow high removal efficiency but not complete (95–99% for cobalt removal) [24], stream with metal concentrations in the ppm range where adsorption is preferred over other techniques [25]. In addition, these metals are released into the environment, in ever-increasing quantities due to their dramatically increasing industrial use. Therefore, the study of the processes to prevent this or to clean up the water is crucial.

In the literature, several authors have studied the heavy metal adsorption onto industrial adsorbents. Those adsorbents show elevated surface areas, large porosity and specific properties designed exclusively for every issue [18]. Thereby, materials like activated carbon [26], zeolites [27], polymeric materials and metallic oxides [18] can reach surface areas over 1000 m^2/g, showing high efficiency in metal removal from aqueous solutions. However, they are quite expensive, or their synthesis is time-consuming and heavily chemical dependent [28]. Nevertheless, it is worth mentioning the existence of natural and low-cost adsorbents, obtained from natural resources, such as clays and natural zeolites, and agricultural and industrial waste and by-products [18], such as shells, wood, coal, fly ash, sludge and sawdust, among others [29]. These adsorbents are mainly untreated with expensive pretreatment processes, and generally they do not require a regeneration process [30]. So that, their low investment costs, simple accessibility, and acceptable effectiveness [31] make them an interesting alternative to the traditionally used adsorbents.

Even though there is a lack of depth investigation involving adsorption mechanisms [18], researchers have examined these low-cost adsorbents, directly studying their potential in the removal of heavy metals from wastewater. The adsorption of some potentially toxic elements has been widely investigated on dolomite, with elements such as strontium, barium [32], cadmium and nickel [33], proving that dolomite is a cheap and effective solid mineral with good adsorption properties [34]. Ivanets et al. conducted adsorption experiments of some heavy metals onto modified phosphate dolomite, reaching removal efficiencies higher than 90% for Fe^{2+}, Pb^{2+} and Cu^{2+} and lesser than 85% for Co^{2+} and Ni^{2+}, for an adsorbent dosage of 10 g/L [35]. El-Sayed et al. evaluated the potential of Egyptian diatomite for the heavy metal removal, controlling the pH, obtaining removal efficiencies over 90% for different cations like Al^{3+}, Ba^{2+}, Cu^{2+} and Pb^{2+} [36]. The Sr^{2+} adsorption onto barium sulphate was studied by Bracco et al, investigating the surface properties of the adsorbent and the influence of metal concentration in the aqueous phase [37].

Apart from the mineral adsorbents named above, it is important to consider the versatility of some widely used adsorbents, such as natural zeolites and activated carbon, to undertake the complete removal of heavy metals from wastewaters. The use of zeolites for cobalt and lithium adsorption has been widely covered. Gupta et al. evaluated the potential of hydroxyapatite/zeolite composites for cobalt adsorption, removing the 63% of initial cobalt (C_i = 5 mg/L) with an adsorbent dosage of 2 g/L [38]. Rodriguez and co-workers evaluated the potential of clinoptilolite, a natural zeolite, for the removal of cobalt from aqueous solutions, achieving acceptable results at 333 K with a dosage of 12 g/L and pH 5.5 [39]. Lithium adsorption onto cationic-modified zeolites have been analysed by Park and co-workers with promising results using K^+ modified zeolite and pH between 5 and 10 [40]. Siddiqui et al. studied the adsorption of cobalt using low-cost mesoporous carbon for the fast removal of Co^{2+}, in a 6 min process time, removing the 95% of initial cobalt with a low dosage (0.3 g/L) and an adsorption capacity of 1.6 mg/g [41].

In this work, the selection of sorbents for the sequential removal of cobalt (Co^{2+}) and lithium (Li^+) from aqueous solutions was studied. The present proposal for a two-stage selective adsorption allows for selective separation of metals, thus facilitating their subsequent recovery at high purity and the reuse of the adsorbents. This is a significant advantage over a single-stage adsorption (non-selective) of the two metals on the same adsorbent. In single-stage, it would be necessary a higher amount of adsorbent due to the non-selective adsorption [42]. Dolomite, diatomite, barite, activated mesoporous carbon, natural and commercial zeolites were evaluated. Characterisation of the sorbents was carried out to allow a better understanding of their properties and behaviour. The sorption experiments were carried out controlling pH, dosage, and initial metal concentration as the main variables of the experiments. Finally, the selectivity towards these metals in bimetallic solutions was studied, with the aim of removing and separating Co^{2+} and Li^+ on different sorbents.

At this point it is interesting to note that due to the nature of some of the adsorbents used, the removal of cations from the aqueous solution was expected to occur by both adsorption and/or ion exchange. Therefore, the term sorption is used since adsorption and ion exchange are sorption operations [43].

2. Experimental

2.1. Chemicals

Silica gel (SiO_2, pore size 150 Å, particle size 75 – 250 μm), supplied by Acros Organics, sucrose ($C_{12}H_{22}O_{11}$, ≥ 99.5%) and hydrofluoric acid (HF, 40%), from Sigma-Aldrich, were used in the activated mesoporous carbon synthesis. Cobalt (II) nitrate hexahydrate ($Co(NO_3)_2{\cdot}6H_2O$ ≥ 98%) supplied by Sigma-Aldrich and lithium chloride (LiCl, 99%), for Alfa Aesar were used for the solution preparation. Sulfuric acid (H_2SO_4, 98%) and ethanol (C_2H_6O, 96% v/v) were purchased to Panreac, nitric acid (HNO_3, 69.5%), supplied by Carlo Erba and hydrochloric acid (HCl ≥ 37%), by Fluka, were employed as well. For the NaY zeolite synthesis, the reactants used were sodium silicate (Na_2SiO_3) and sodium hydroxide (NaOH), by Panreac and sodium aluminate ($NaAlO_2$) supplied by Carlo Erba. Deionized water was used throughout.

2.2. Sorbents

Dolomite ($CaMg(CO_3)_2$) and barium sulphate ($BaSO_4$) were provided by Minerals MIVICO Company. Diatomite ($SiO_2{\cdot}nH_2O$) and 13X zeolite, in powder, were supplied by Sigma-Aldrich. Natural zeolite

clinoptilolite (CLP) from Zeocat Soluciones Ecológicas, commercial 13X zeolite, in pellets, by CECA and commercial USY zeolite, supplied by Grace Davison were used as well. Apart from the clinoptilolite and 13X zeolite, in pellets, all the sorbents were supplied in powder form.

NaY zeolite synthesis was carried out via the hydrothermal method, according to previous works of the laboratory group [44]. Activated mesoporous carbon (DMC) synthesis was performed following the replica method, according to previous works [45].

2.3. Characterization

X-ray diffraction (XRD) patterns were recorded on a SIEMENS-D501 diffractometer with CuKα1 radiation for 2θ between 5° and 50° scanning range and a step size of 0.1. Surface chemistry of the sorbents was analyzed by Fourier Transform Infrared Spectroscopy (FTIR) in the Spectroscopy and Correlation Unit of Universidad Complutense de Madrid. A Nicolet iS50 FTIR spectrophotometer, in the infrared spectrum (400–4000 cm^{-1}) was used. Zeta potential measurements were carried out using a Zetasizer Nano ZS apparatus, provided by Malvern Instruments. Zeolites chemical composition was determined by X-ray fluorescence (XRF) using a PHILIPS PW-1480.

N_2 adsorption–desorption isotherms at 77 K were obtained by using a Micromeritics ASAP-2020 apparatus. Surface area and pore volume were determined using the Brunauer-Emmett-Teller (BET) equation and the single point method, respectively. To obtain the microporous surface area (S_{micro}) and microporous volume (V_{meso}) the *t*-plot method was used.

2.4. Sorption experiments

Sorption experiments were carried out in batch mode, using a Thermomixer Confort shaker with orbital agitation by Eppendorf. The experiments were performed in Eppendorf tubes, adding the required amount of sorbent and 2 mL of metal (cobalt or lithium) solution, prepared from the corresponding salt. After the sorbent and the adsorbate were put in contact with agitation and the equilibrium was reached, the sorbent was separated from the aqueous solution by centrifugation and filtration to remove the sorbent leftovers. The pH was controlled throughout the experiment since metals may precipitate depending on the value of the pH. Lithium and cobalt concentration were analyzed using an AA-7000 Shimadzu atomic absorption spectrophotometer. Each measurement was performed by triplicate, being the error ± 2%. The selected parameters to evaluate the sorption process were the sorption capacity (q) and the percentage of metal sorbed respect to the initial concentration. They were calculated by mass balance according to the equations (1) and (2).

$$q = \frac{(C_0 - C) \bullet V}{m} \quad (1)$$

$$\%M^{+}_{adsorbed} = \frac{(C_0 - C)}{C_0} x100 \quad (2)$$

Where q (mg/g) is the sorption capacity, C_0 y C (mg/L) relates to the metal concentration in the liquid phase, at zero time and at t time, respectively; m (g) is the mass of the sorbent and V (L) is the sample volume. The kinetic sorption curves were obtained by measuring the metal concentration in the solution, at different times. The points of the curve were prepared by weighing the desired amount of carbon and adding 2 mL of metal solution in each tube. Then, the tubes were removed from the shaker at corresponding times, then centrifuged and filtered. Sorption isotherms were obtained similarly.

Selectivity sorption experiments were performed in batch mode, using a Hettich Thermomixer MHR thermoblock. The required amount of sorbent was added to the tubes, with 20 mL of a bimetallic cobalt-lithium solution. Reaching the equilibrium, the solid and the fluid phase was separated by centrifugation and filtration. The liquid part was collected for analysis. For the selectivity experiments performed in sequential operation the second step was carried out by collecting a liquid sample from every point of step one and put it in contact with the other sorbent.

3. Results and discussion

Materials that can be used as sorbents are diverse, with different chemical and surface properties, some of which can be modified to improve their sorption capacity. Considering their different characteristics, a selective separation of some metals from a solution would be possible using sorption. The correct selection of the sorbent is crucial to achieve a great interaction between sorbent and adsorbate, especially when working with multimetallic solutions, improving the mass transfer, maintaining the properties of the sorbent, and allowing a proper separation.

3.1. Sorbent characterization

Fig. 1 shows the X-ray diffraction patterns of zeolites (Clinoptilolite, USY, NaY and 13X) and dolomite. The XRD profiles of USY, NaY and 13X showed the characteristic peaks of the FAU framework which coincide with those obtained for the commercial zeolite NaX supplied by Sigma-Aldrich (13X powder). The clinoptilolite used showed the typical mineralogical diffraction pattern of a HEU framework topology, with some impurities. Finally, the dolomite also showed a high intensity in the characteristic peak at 31° (2) indicating high crystallinity.

Tables 1 and 2 display the textural characterization of the sorbents. The BET surface area of the natural mineral sorbents (dolomite, diatomite, and barite) was quite low, between 2–4 m^2/g, being the majority external surface area. Zeolites showed a much larger surface area (600–900 m^2/g), predominantly microporous (≈ 95% in FAU zeolites). Clinoptilolite (CLP), the natural zeolite employed in this study, presented a smaller surface area than the other zeolites. Activated mesoporous carbon presented lower surface area than the zeolites (<400 m^2/g), but mostly mesoporous area (≈80%) with a wide pore size distribution in the mesoporous range, with an average pore size of 270 Å, and 92% mesopore volume.

For zeolites, since ionic exchange is the predominant process, a key parameter is the silicon/aluminum molar ratio. The aluminum presence involves a negative charge deficiency in the structure of the zeolite. This deficiency shall be compensated with other cations, such as sodium and potassium. The closer to one this ratio is, the greater the number of negative charges the zeolite has, so the sorption sites available for cation sorption will be greater. Table 3 shows the Si/Al molar ratio for all

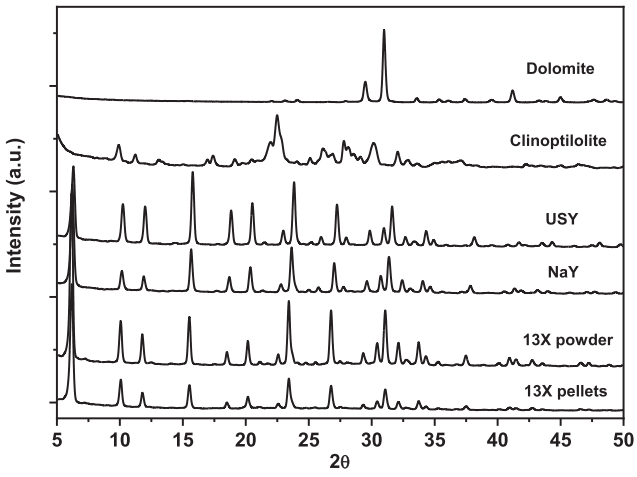

Fig. 1. XRD patterns of the FAU zeolites (USY, NaY and 13X), Clinoptilolite and Dolomite.

Table 1
Textural characterization of the natural and carbonaceous sorbents.

	Natural			Carbonaceous
	Dolomite	Barite	Diatomite	Activated mesoporous carbon
S_{BET} (m^2/g)	3,8	3,2	2,2	365
S_{micro} (m^2/g)	–	–	–	74
S_{meso} (m^2/g)	3.8	3.2	2.2	291
V_{pore} (cm^3/g)	0.008	0.008	0.002	0.89
V_{micro} (cm^3/g)	–	–	–	0.07
V_{meso} (cm^3/g)	0.008	0.008	0.002	0.82

Table 2
Textural characterization of the zeolites.

	USY	NaY	13X powder	13X pellets	CLP
S_{BET} (m^2/g)	782	852	877	660	25
S_{micro} (m^2/g)	722	814	842	626	2
S_{meso} (m^2/g)	60	38	35	34	23
V_{pore} (cm^3/g)	0.334	0.347	0.336	0.349	0.148
V_{micro} (cm^3/g)	0.271	0.305	0.313	0.233	0.002
V_{meso} (cm^3/g)	0.063	0.042	0.023	0.116	0.146

Table 3
Si/Al molar ratio of the zeolites.

	USY	NaY	13X powder	13X pellets	CLP
Si/Al molar ratio	3.1	2.5	1.3	1.4	6.1

zeolites. X zeolites (13X powder and 13X pellets) showed the lowest ratio, near to the unit, while Y zeolites (USY and NaY) showed a higher ratio value, especially the USY zeolite which suffered a dealumination process. Clinoptilolite, with a different structure (HEU type), presented the highest ratio in 6.1. It can be concluded that 13X zeolites will have the highest sorption potential a priori.

Fig. 2 shows the FTIR spectra of one of the natural sorbents employed, the dolomite (2A) and the activated and non-activated mesoporous carbon (2B). FTIR dolomite spectra showed the characteristic bands of CO_3^{2-} groups, at 1430 cm^{-1}, 848 cm^{-1} and 728 cm^{-1}. The broad absorption band in the 3600–3300 cm^{-1} spectral region was associated to the stretching and bending vibrations of adsorbed water. [46]. Analyzing the spectrum of the carbonaceous materials, the band at 3400 cm^{-1} was associated to the O-H stretching corresponding to the OH^- ions present in phenolic groups [47]. The band located at 2900 cm^{-1} was associated to the C-H vibrations of aromatic and aldehyde groups. The small depression at 2360 cm^{-1} was assigned to the presence of -COOH groups. For the non-activated mesoporous carbon, the peak located a 1630 cm^{-1} was associated to C=C stretching. However, for the activated mesoporous carbon this peak was shifted to 1600 cm^{-1}, with greater intensity, and was associated to the C=O axial deformation in carboxyl acids [48]. The activated mesoporous carbon also presented a new peak located a 1700 cm^{-1}, again associated to the C=O groups existent in aldehydes, ketones and quinones groups [49]. Finally, the band at 1100 cm^{-1} was related to the C-O stretching of phenolic or alcoholic groups [45].

The activation of the carbon (Fig. 2B) involved two important differences regarding the FTIR spectra. The presence of new absorption bands, in the spectral region in 1720 and 1600 cm^{-1}, were observed, associated to C=O stretching. On the other hand, the increase in the intensity of the existing ones was also noticed. The activation process under oxidizing conditions mainly increased the presence of carboxylic [50] and phenolic groups [51]. Their presence resulted in an increase in the negative charge density, hence, their potential in the metallic cations

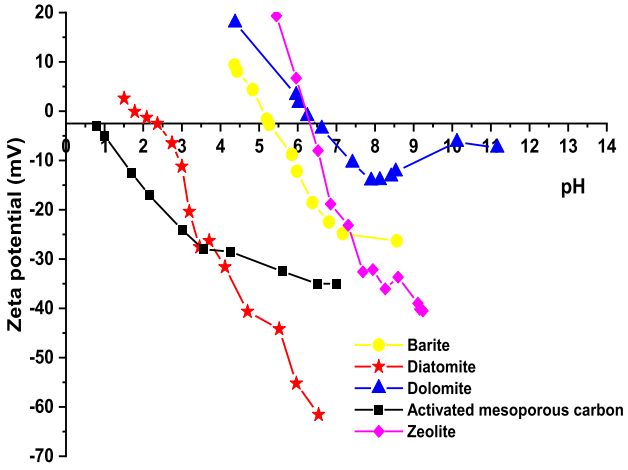

Fig. 3. Zeta potential of natural sorbents, zeolite and activated mesoporous carbon.

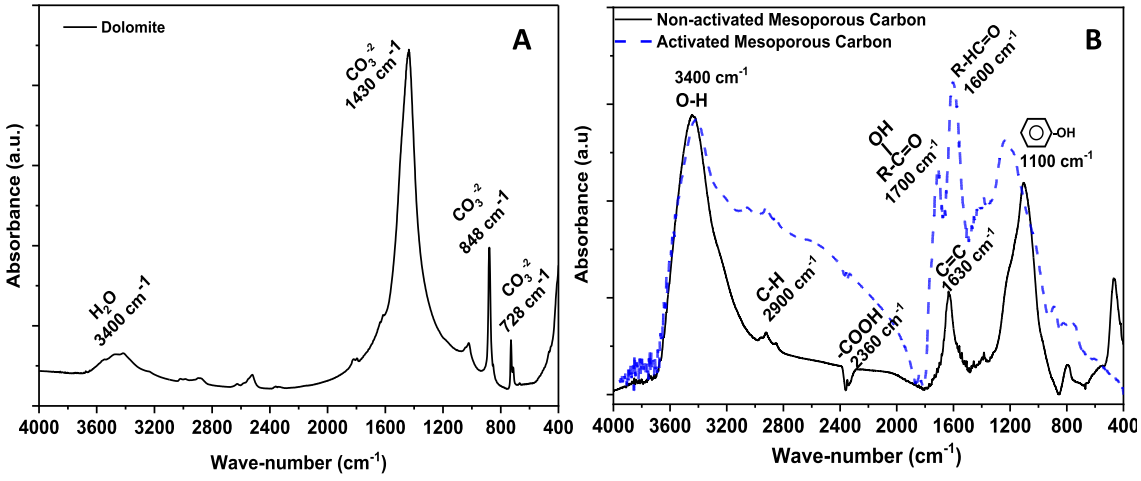

Fig. 2. FTIR spectra of dolomite (a) and activated and non-activated mesoporous carbon (b).

sorption.

Fig. 3 shows the results of the zeta potential measurement. This technique can be used as a predictive tool to understand the electrostatic interactions between the adsorbate and the sorbent material [52]. The initial analysis revealed the presence of an isoelectric point (IEP) for the natural materials ($IEP_{dolomite} = 6.5$, $IEP_{diatomite} = 2.3$, $IEP_{barite} = 5.2$). Consequently, if the operational pH falls below pH_{IEP}, the sorbent will be positively charged, which will affect to the electrostatic interactions between the cations and the surface sorption sites. Concerning the activated mesoporous carbon, it showed no isoelectric point, the potential remained negative in the pH range studied, reaching a minimum of –35 mV at 7 pH. In the case of the zeolites, they showed an $IEP_{zeolite}$ of 6.1. According to this analysis, the sorbent whose zeta potential is more negative at the operational pH (below 8) should be, a priori, the one with the highest driving force for the sorption of cations like Co^{2+} or Li^{+}. However, while this is important, there are other effects to consider. The pH also affects to the complex ions that can be formed in aqueous solution and, by extension, the whole sorption process. This can be explained by the speciation in aqueous solution of the studied metals, Co^{2+} and Li^{+}. The variation of the Co^{2+} concentration depending on the pH was analyzed in detail. At pH 8, the precipitation of Co^{2+} as $Co(OH)_2$ begun, gradually decreasing the initial concentration (40 mg/L). At pH 8.6, the concentration had decreased a 17%. These results confirmed the evidence studied by Krishman et al, wherein a developed cobalt speciation diagram showed how this metal gradually begins its precipitation at pH over 8 [53]. For lithium, precipitation as Li(OH) was studied. The pH range analyzed was from 6.2 to 13, and it was found that at pH 12.8 the concentration decreased by 7%, decreasing a 13% at pH 13. So, pH 13 can be labeled as the point where the precipitation is significant, so it is desirable to work below this value in the sorption process.

Since pH is a critical parameter in the sorption process, affecting both the interaction between sorbent and adsorbate and the precipitation of this metals as hydroxide species, the variation of the pH when the sorbent was in suspension was studied. Dolomite, diatomite, and barite showed a basic behavior in aqueous suspension. Working with dosages between 1 and 12 g/L, suspension pH raised to values over 8 (10 for dolomite, 9 the diatomite and 9 for barite). This basic character can be explained by the following reactions of releasing OH^{-} ions into solution:

Dolomite:

$$(CaMg(CO_3)_2)_{solid} + H_2O \leftrightarrow Ca^{2+}_{(aq)} + Mg^{2+}_{(aq)} + 2(CO_3)^{2-}_{(aq)} \quad (3)$$

$$2(CO_3)^{2-}_{(aq)} + 2H_2O \leftrightarrow 2HCO^{-}_{3(aq)} + 2OH^{-}_{(aq)} \quad (4)$$

Barite:

$$(BaSO_4)_{solid} + H_2O \leftrightarrow Ba^{2+}_{(aq)} + SO^{2-}_{4(aq)} \quad (5)$$

$$SO^{2-}_{4(aq)} + 2H_2O \leftrightarrow HSO^{-}_{4(aq)} + OH^{-}_{(aq)} \quad (6)$$

The equilibrium reactions abovementioned are strongly shifted to the solid side, because of the low solubility of these compounds in water. The solubility product of the dolomite is extremely low [54] and ranges from 10^{-17} to 10^{-19} [55]. This means that the reaction occurs to the left and the solid form of the mineral remains intact. However, the dissolved amount was enough to increase the pH. For the barite, its solubility product constant is also relatively low, $1.08 \cdot 10^{-10}$ at 25 °C [56], which also explains its low solubility. Diatomite also has a low solubility in water (<0.001 g/L) [57].

Carbonaceous materials such as activated mesoporous carbon are well known for their acidity. Some acid groups like the phenolic ones behave as an acid in solution, giving H^{+} to the system by dissociation (pKa = 9.95). On the contrary, quinone, ketone and aldehyde groups present in the activated mesoporous carbon does not acidify the system by not being able to give protons [51]. Regarding the zeolites, they showed an alkaline behavior in aqueous media, increasing the pH over 11. This was due to protons cationic exchange, which increased the presence of OH^{-} anions in the media. 13X pellets zeolite and clinoptilolite (CLP) kept the aqueous media at neutral pH, because of the presence of the binder used in the 13X pellets and the greater Si/Al molar ratio in the clinoptilolite.

3.2. Cobalt sorption

Cobalt sorption kinetics were performed firstly on the natural sorbents, dolomite, diatomite, and barite. Since pH increased when the sorbents were added to the aqueous media, low sorbent dosage had to be used. Fig. 4 shows the results of these experiments. With this selected dosage, the pH of the experiment was between 6 and 8 for the dolomite, 6–7.5 for the barite and 6–7.3 for the diatomite. These values also allowed the operation above the isoelectric point during the whole process. The cobalt removal was very low using barite and diatomite, with sorption capacities of 0.4 and 0.15 mg/g, respectively. However, using dolomite, the removal was successfully superior, close to the 65%, with a sorption capacity at equilibrium of 5.8 mg/g. Cobalt removal using natural and low-cost sorbents is attractive for their easy accessibility and direct use without pre-treatments. Their sorption capacity was strongly dependent on the interactions between their surface groups and the Co^{2+} ions [18]. Dolomite can easily incorporate Co^{2+} to its structure, up to 20 mol% in the form of $Ca(Mg,Co)(CO_3)_2$ [58]. Divalent cation sorption onto dolomite can be explained as an ion exchange process in the interphase S-L. The ionic exchange of Co^{2+} by Mg^{2+} was possible since the charge and the ionic radius of both metals are very similar (Co^{2+} = 0.63 Å and Mg^{2+} = 0.65 Å). Those similar characteristics, along with a compressed octahedral coordination (relative to Mg^{2+} coordination) enables to reduce the energy of the complex, making stable structures [59]. On the other hand, the ionic exchange by Ca^{2+} ions may also occur since the charge is the same, even though ionic radius is larger (0.99 Å) [60]. In this sense, Kornicker et al. showed that Co^{2+} can be significantly sorbed on calcite, one of the two carbonates present in dolomite [61]. In the dolomite used in this work, as the Ca/Mg molar ratio was 4.2, the ion exchange was predominantly by Ca^{2+} ions. On the other hand, the cobalt ions can also be incorporated to the surface by interaction with the CO^{2-}_3 anions at the edge of the rhombohedral structure. This is a highly pH dependent process since the hydrogen ions can interfere in the complex formation due to their affinity to the ionic exchange sites [59]. Therefore, Co^{2+} showed a significant affinity for the surface of dolomite.

Once the sorption of cobalt on the natural materials was studied, the

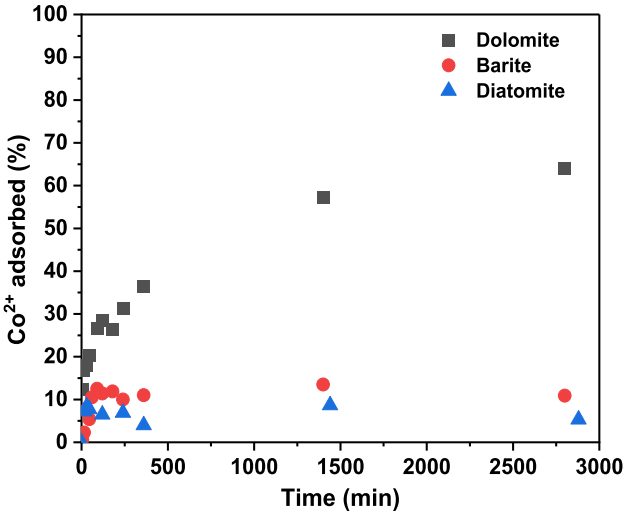

Fig. 4. Cobalt sorption kinetics onto dolomite, diatomite, and barite. Conditions: $[Co^{2+}]$ = 20 mg/L, T = 25 °C, speed = 1100 rpm, dolomite dosage = 2 g/L, barite dosage = 6 g/L, diatomite dosage = 10 g/L.

synthesized materials like the activated mesoporous carbon and the NaY zeolite, and the commercial ones, 13X powder and pellets, USY and CLP were employed. Apart from the 13X pellets zeolite, the rest of the zeolites increased the pH of the suspension over 8 (even at low doses), so cobalt sorption was not possible on them. Commercial 13X pellets zeolite kept the suspension pH near 7.5, so precipitation was not troublesome. Activated and non-activated mesoporous carbon acidified the media, keeping the pH in values around 3.5. Fig. 5 shows the cobalt sorption kinetics with these materials.

Cobalt removal with the abovementioned sorbents was clearly superior to the obtained with the natural sorbents. These materials allowed to work with higher dosage since pH was not a problem. Activated mesoporous carbon removed over the 85 % h the, with a capacity of 1.6 mg/g and 13X pellets zeolite removed over the 95% (q = 1.9 mg/g). Non-activated mesoporous carbon barely adsorbed cobalt, only a 3% of initial value (q = 0.04 mg/g). The activation of the carbon provided the oxygenated groups, mostly carboxyl and phenolic (Fig. 2B) needed for cobalt sorption [62]. Those groups stood out for their negative charge density, which promoted the Co^{2+} sorption for two mechanisms [63]. First, cobalt ions in dissolution can replace the H^+ ions present in the acidic oxygenated groups of the surface of the carbon. That sorption process decreased the pH of the system. Besides, Co^{2+} ions can additionally be adsorbed onto aromatic rings by cation-π interactions. It is interesting to emphasize the mesoporous character of the synthesized activated carbon, whose pore size distribution belongs to the mesopore range. Consequently, the sorption process was considerably faster (equilibrium time less than 10 min), especially for small molecules, due to the non-existence of diffusion limitations. This was the case of the hydrated cobalt $[Co(H_2O)_6]^{2+}$ whose hydrated solvation shell diameter is 8.46 Å [64], significant smaller than the activated mesoporous carbon pore size (approximately 270 Å).

With zeolites as sorbents, 4 h were necessary to complete the equilibrium, due to their microporous structure [27]. Cobalt can access the cationic sites of the FAU structure but releasing its solvation shell, being the relevant parameter the cobalt ionic radius, 0.63 Å, and the low Si/Al molar ratio of the zeolite (1.4).

3.3. Lithium sorption

Once performed the monometallic sorption experiments with cobalt, sorption with lithium alone in the solution was carried out. Fig. 6 displays the lithium sorption experiments on dolomite, activated and non-activated mesoporous carbon.

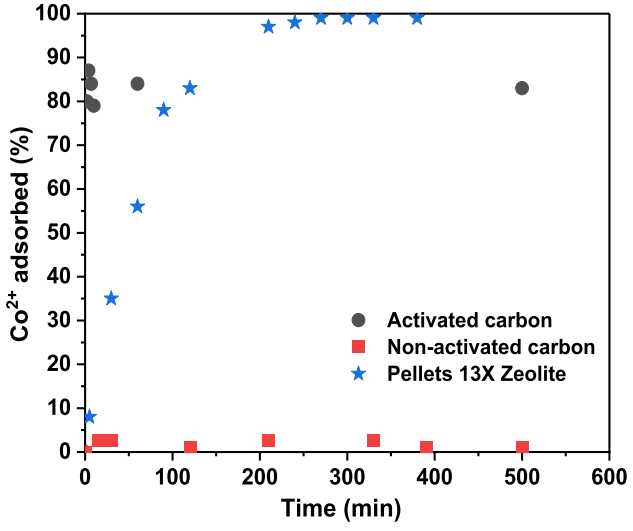

Fig. 5. Cobalt sorption kinetics onto activated and non-activated mesoporous carbon and 13X zeolite (pellets). Conditions: $[Co^{2+}]$ = 24 mg/L, T = 25 °C, speed = 1100 rpm, sorbent dosage = 12 g/L, initial pH = 6.

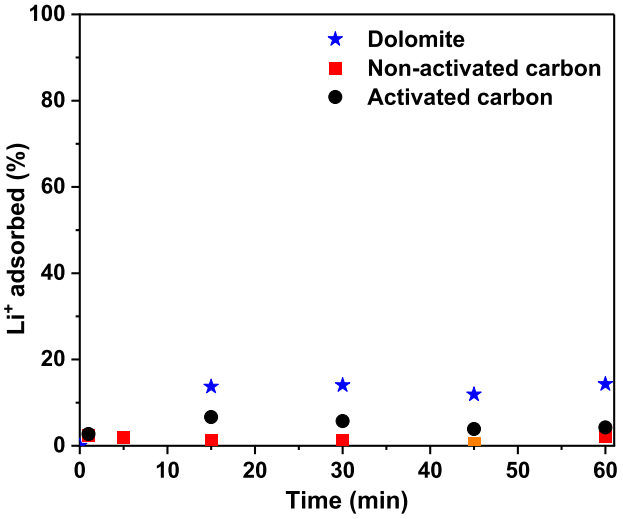

Fig. 6. Lithium sorption kinetics onto dolomite, activated and non-activated mesoporous carbon. Conditions: $[Li^+]$ = 20 mg/L, T = 25 °C, speed = 1100 rpm, dolomite dosage = 2 g/L, carbon dosage = 12 g/L.

Regarding lithium sorption, pH was not a problem, since according to the precipitation study, lithium did not start precipitation until pH close to 13, which did not occur throughout this sorption process. None of these three sorbents reached a significant lithium removal. Sorption was insignificant, only 2.3% of removal was reached with the non-activated mesoporous carbon and 6.3% with the activated one. This was due to the low molecular weight (MW = 6.9) and low charge (+1) of lithium, along with the small hydrated ionic radius (3.82 Å) [65]. The driving force and the electrostatic interaction between the lithium ions and sorption sites will be significantly lower than that of cobalt. Onto activated mesoporous carbon, lithium sorption capacity (0.1 mg/g) was 16 times lower than cobalt sorption capacity. Therefore, it can be stated that the selective separation of these two metals is affordable with activated mesoporous carbon.

With dolomite as sorbent, lithium removal reached 12%, being the sorption capacity 3.6 times lower than the sorption capacity of cobalt. The lower valence of this metal reduced and weakened the ionic interactions between this cation and the dolomite surface sites, so that the sorption capacity was relatively low. The incorporation of cations into the structure of carbonate minerals is partially prevented for monovalent (such as Li^+) and trivalent cations, due to charge imbalances and ionic radius differences with the cations present in dolomite values exhibit a strong pH dependence. For experiments conducted at similar growth rates (i.e. Rate = 10–7.7 ± 0.2 mol m^{-2} s^{-1}), DLi [66]. This behavior does not happen with divalent ions like Co^{2+} as it was addressed before, where the mechanism approaches direct and ideal substitution [67].

Fig. 7 displays the lithium sorption on the different FAU and HEU zeolites. For all the zeolites the sorption process was very fast, almost instantaneous since the predominant process was ion exchange. Those FAU zeolites whose Si/Al molar ratio was low (<1.5), 13X pellets and powder zeolites, showed higher lithium removal, upper 70%. However, CLP zeolite, (Si/Al molar ratio 6.1), only showed a 20% of lithium removal. In addition of the low Si/Al molar ratio, FAU framework is more open and accessible (7.8 Å) than HEU framework of clinoptilolite (with parallel channels and rings of 2.8 × 4.7 Å, 3.6 × 4.6 Å and 3.1 × 7.5 Å size) [68]. A low Si/Al molar ratio promotes the ionic exchange, because of the large number of negative charges inside the structure. This negative charge density occurs because of the isomorphic substitution of Si^{4+} for Al^{3+}, which maximizes the ion exchange capacity between lithium and the zeolite synthesis cations (Na^+). In the HEU

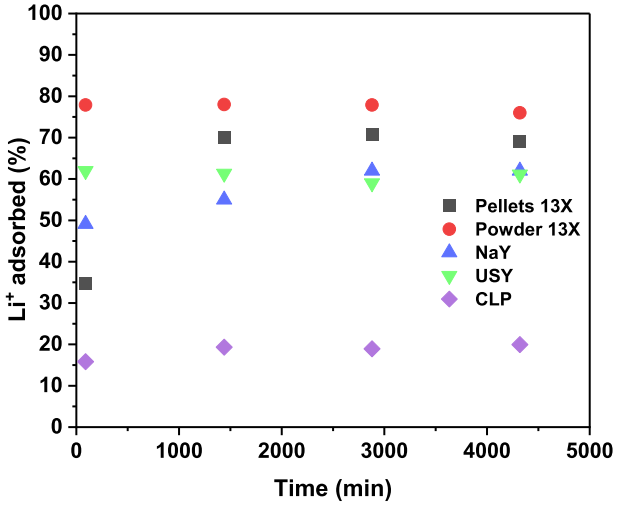

Fig. 7. Lithium sorption kinetics onto zeolites. Conditions: [Li^+] = 20 mg/L, T = 25 °C, speed = 1100 rpm, sorbent dosage = 12 g/L, initial pH = 6.5 (pellets 13X and CLP), 8.3 (USY), 10.5 (NaY) and 11 (powder 13X).

framework (CLP), the one with the lesser lithium sorption, the silicon/aluminum molar ratio was 6.1, which decreased the yield of the ion exchange process. Furthermore, according to Table 1, this zeolite presented the lowest surface area, in consequence the lowest sorption capacity. The pH of the medium remains around 10–11 for powdered zeolites. However, the USY zeolite kept the system at a lower pH, around 9, as it was in protonated form. The zeolites with binder (13X and CLP pellets) kept the pH at neutral values, close to 7, throughout the experiment.

3.4. Sorption isotherm

Fig. 8 shows the sorption isotherms at 25 °C of cobalt onto dolomite and activated carbon. Sorption isotherms can be classified as L2 type, according to the Giles classification [69]. The L-shaped curve is a typical sorption isotherm for dilute solutions on a solid/liquid interface. As for the subgroup, type 2 indicates that the adsorbent surface is complete and therefore presents a plateau. Dolomite reached a maximum sorption capacity of around 14 mg/g while for activated carbon it was lower, about 5 mg/g.

Fig. 9 displays the sorption isotherm at 25 °C of lithium onto 13X zeolite. The behaviour was similar to that of cobalt sorption in the previous sorbents. The shape of the isotherm corresponded to an L2 type, reaching a maximum sorption capacity of around 6 mg/g.

3.5. Sorption of cobalt and lithium in bimetallic solutions

Previous studies allowed us to establish sorbent sets that can achieve selective removal of cobalt and lithium. Among the sorbents studied, dolomite and activated mesoporous carbons adsorbed cobalt but not lithium. However, only zeolites with FAU structure were able to remove lithium significantly. Activated mesoporous carbon presented a ratio (% Co removed) / (% Li removed) above 12, showing a potential for the selective separation of cobalt and lithium. To a lesser extent, dolomite also showed potential for selective separation, with a (% Co removed) / (% Li removed) ratio over 4. Therefore, combining activated mesoporous carbon or dolomite and a FAU zeolite would be desirable to selectively remove lithium and cobalt from the aqueous solution.

Firstly, the sorption over activated mesoporous carbon and FAU zeolite was carried out with a bimetallic solution containing cobalt and lithium. 13X zeolite (pellets) was used as the pH of the medium was below 8, ensuring that cobalt removal took place by sorption avoiding precipitation. The initial concentrations used for this experiment were proportional to those existing in a cobalt and lithium recovery leachate, [Co^{2+}] = 24 mg/L and [Li^+] = 6 mg/L [13]. Fig. 10 displays the percentage of removal of both metals by sorption.

The pH during sorption was kept below 8, with an initial pH of 5.6 and a final pH of 7.6. As it can be seen in Fig. 10 cobalt sorption was over 90%, whereas for lithium the removal was below 50%. This behavior was different from that observed in the experiments with monometallic solutions, displayed in Fig. 7, where 76% of the initial lithium was removed using 13X zeolite (pellets). This removal decreased by 40% when Co^{2+} was also present in the solution. This decrease was due to the competitiveness between cobalt and lithium for the sorption sites, mainly in the zeolite, since Co^{2+} can be adsorbed on both sorbents. Therefore, a complete separation of both metals was not reached.

To reduce this competitive effect and to successfully separate both cations, the sorption process was carried out sequentially. Firstly, sorption of cobalt was carried out using only activated mesoporous carbon (1^{er} stage). Then, after separating the activated mesoporous

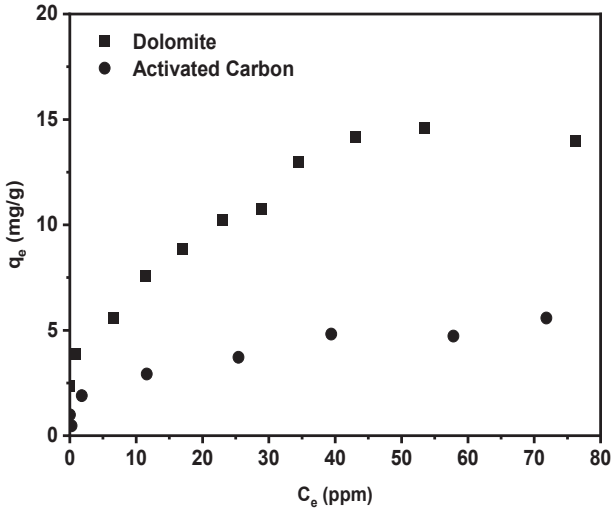

Fig. 8. Sorption isotherm of Cobalt onto dolomite and activated carbon at 25 °C. Conditions: speed = 1100 rpm, dolomite dosage = 2 g/L, activated carbon dosage = 12 g/L.

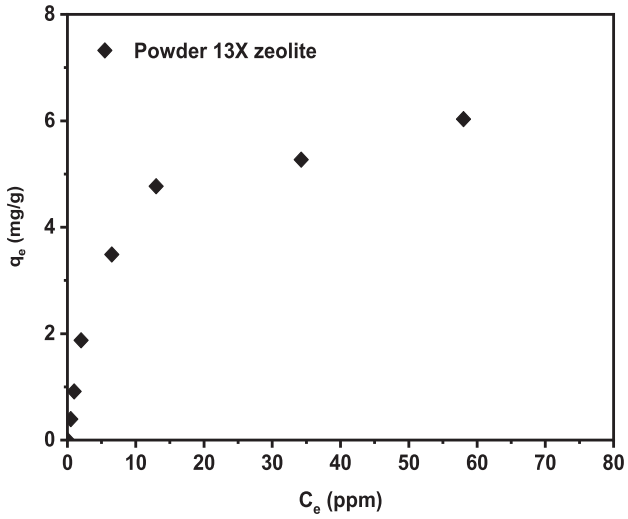

Fig. 9. Sorption isotherm of Lithium onto powered 13X zeolite at 25 °C. Conditions: speed = 1100 rpm, dolomite dosage = 2 g/L, activated carbon dosage = 12 g/L.

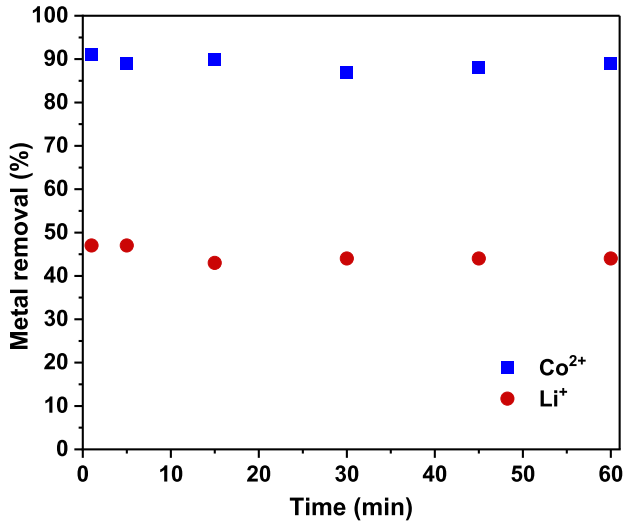

Fig. 10. Cobalt and lithium simultaneous sorption results onto activated mesoporous carbon and 13X zeolite (pellets). Conditions: $[Co^{2+}]$ = 24 mg/L, $[Li^{+}]$ = 6 mg/L, T = 25 °C, total sorbent dosage = 12 g/L, speed = 650 rpm.

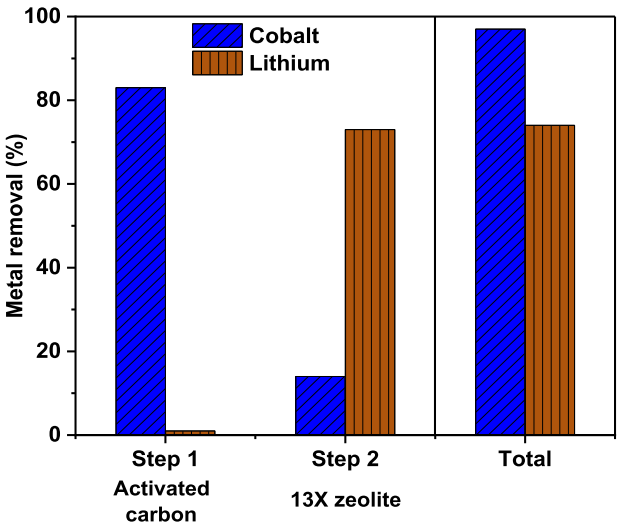

Fig. 12. Cobalt and lithium sequential sorption results onto activated mesoporous carbon and 13X zeolite (powder). Conditions: $[Co^{2+}]$ = 24 mg/L, $[Li^{+}]$ = 6 mg/L, T = 25 °C, carbon dosage = 12 g/L, zeolite dosage = 12 g/L, speed = 650 rpm, sorption time = 24 h (step 1), 48 h (step 2).

carbon, 13X zeolite (powder) was used to remove the remaining lithium in the solution (2nd stage). Fig. 11 shows a schematic of the sequential process, with the two experiments carried out, the first with activated mesoporous carbon/13X zeolite and the second with dolomite/13X zeolite, which will be explained later.

The sorption of the two metals on different sorbents would result in a selective separation allowing their subsequent recovery by desorption at high purity. The results of the first sequential experiment are shown in Fig. 12.

The initial pH was 6.1, decreasing drastically to 3.1 during the first stage of the experiment (sorbent: mesoporous activated carbon), and after centrifugation and filtration, in the second stage (sorbent: zeolite 13X powder), the pH increased to 8.5 due to the basic character of the zeolite in aqueous suspension. Nevertheless, this was not a problem for the sorption of lithium. In this way, it was possible to remove firstly 83% of cobalt over activated mesoporous carbon (1.8 mg/g) with an insignificant removal of lithium. In the next step, the zeolite allows to achieve a 75% lithium removal. However, part of the cobalt eliminated in the second stage was removed by precipitation as the pH reached a value of 8.5.

The other selective sorbent was the dolomite. Similar sequential sorption experiment (Fig. 11) was carried out using dolomite and 13X zeolite (powder) to remove cobalt and lithium respectively. However, to study the sorption of cobalt on dolomite, it was necessary to work at a pH below 8, but dolomite, at the dose of the experiment (12 g/L), increased the pH above this value. To keep the pH below 8 a solid phase pH buffer (*solid buffer*) was used in order not to increase the ionic strength of the medium. For this purpose, non-activated mesoporous carbon was used, as it did not show sorption capacity for either cobalt or lithium, and it decreased the pH of the solution medium due to its acid behavior in aqueous suspension. The combination of non-activated mesoporous carbon and dolomite in a 4:1 weight ratio allowed the pH of the medium to be controlled below 8. The initial pH of the suspension was 6.3, and throughout the experiment it remained stable between 6.3 and 6.6. Therefore, it was possible to control the pH of the sorption medium with the *solid buffer* consisting of a "*basic solid*" such as dolomite and an "*acid solid*" such as non-activated mesoporous carbon, where only one (dolomite) adsorbed cobalt. The results are showed in Fig. 13.

In the first step, dolomite showed a clear selectivity towards cobalt, reaching almost complete removal at 24 h, since the dose was higher than in the monometallic experiments. On the other hand, lithium removal was only 12%. The sorption capacity of cobalt was 1.9 mg/g (32 times higher than that of lithium). Since all cobalt was removed, in the second stage it was possible to work at a pH higher than 8 (pH 11) and to use a 13X zeolite (powder), which had a higher lithium sorption capacity (lower Si/Al molar ratio). In the second step, 85% of the lithium was removed using that 13X zeolite. Therefore, by combining the use of

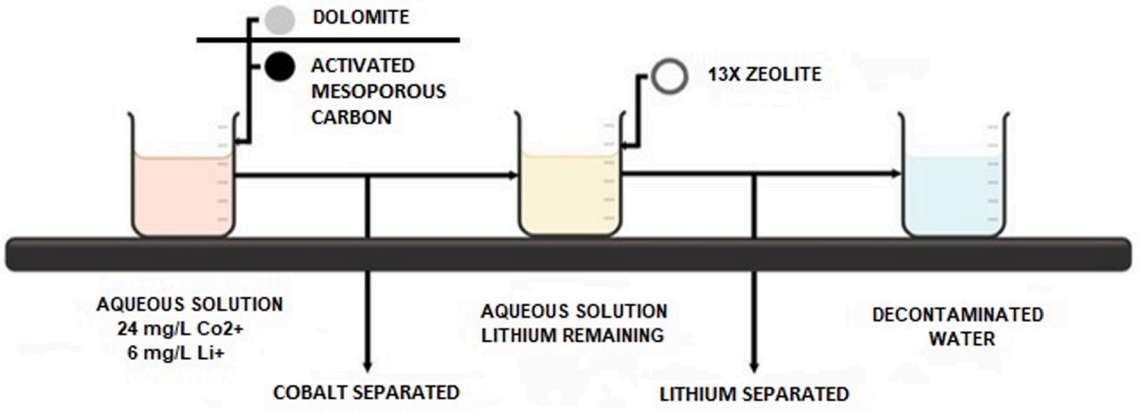

Fig. 11. Sequential selective sorption experiments scheme.

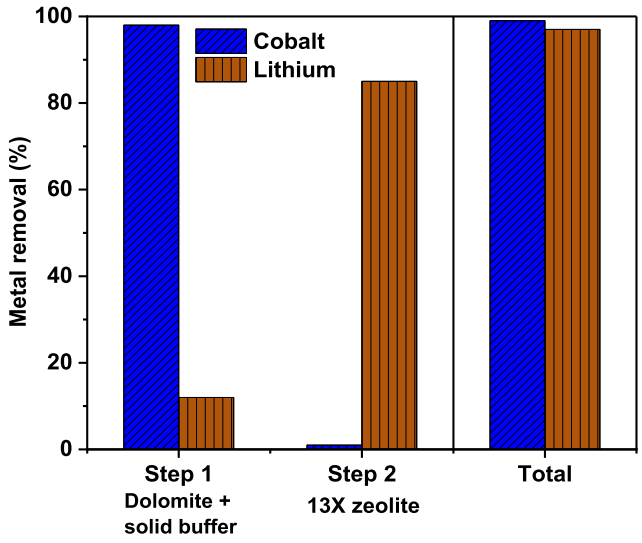

Fig. 13. Cobalt and lithium sequential sorption results onto dolomite and 13X zeolite (powder) (b). Conditions: $[Co^{2+}] = 24$ mg/L, $[Li^{+}] = 6$ mg/L, T = 25 °C, dolomite dosage = 12 g/L, solid buffer dosage = 48 g/L, zeolite dosage = 12 g/L, initial pH = 6.28, speed = 650 rpm.

dolomite and 13X zeolite, a successful selective removal of Co^{2+} and Li^{+} was achieved. The use of a *solid buffer* consisting of a sorbent (dolomite) and a non-sorbent solid (non-activated mesoporous carbon) allowed to keep the pH below 8.

Sequential sorption successfully demonstrated the possibility of achieving a selective separation of these two metals (cobalt and lithium) from aqueous solutions using the right set of materials. The presence of cobalt and lithium on different sorbents means a selective separation that facilitates their subsequent recovery. On the other hand, metals sequential sorption from real wastewater would make possible to achieve one of the Sustainable Development Goals: clean water (6th SDG) by removing these pollutants from water.

4. Conclusions

Cobalt and lithium were successfully separated from a bimetallic aqueous solution. The pH of the medium was a crucial factor that affects sorption process, as cobalt precipitates at pH above. Therefore, the dosage of each sorbent conditions the sorption process. Sorbent set selection can be carried out by sorption with monometallic solutions. The non-activated mesoporous carbon did not adsorb cobalt nor lithium. Therefore, activation of the mesoporous carbon was necessary to obtain sorption capacity. Dolomite, a natural and low-cost material, and mesoporous activated carbon, a material synthesized, removed cobalt but not lithium. On the other hand, only zeolites with FAU structure removed lithium significantly (around 80%). Therefore, mesoporous activated carbon with a ratio of Co^{2+} sorption capacity to Li^{+} sorption capacity of 16, and dolomite with a ratio of 4 were the sorbents that allowed selective separation. Sequential sorption using dolomite, as sorbent to remove cobalt, in the first stage and 13X zeolite, to remove lithium, in the second stage, allows the selective complete separation of both metals. This will enable their subsequent recovery with a high degree of purity. The mixture of dolomite and non-activated mesoporous carbon (inactive as sorbent) acts as a solid phase pH buffer (*solid buffer*), which controls the pH during cobalt sorption around 6.5. This allows working with high doses of dolomite, improving the removal of cobalt from the bimetallic solution.

CRediT authorship contribution statement

N. Conte: Investigation, Methodology, Formal analysis, Writing – original draft. **J.M. Gómez:** Conceptualization, Methodology, Formal analysis, Writing – original draft, Writing – review & editing, Funding acquisition. **E. Díez:** Writing - review & editing. **P. Sáez:** Investigation, Formal analysis. **J.I. Monago:** Investigation, Formal analysis. **A. Espinosa:** Investigation, Formal analysis. **A. Rodríguez:** Writing - review & editing.

Declaration of Competing Interest

The authors declare that they have no known competing financial interests or personal relationships that could have appeared to influence the work reported in this paper.

Acknowledgment

The authors thanks to the Correlation Spectroscopy Research Centre of the Complutense University of Madrid for helping with the characterization. We also thank the companies Minerals MIVICO and Zeocat Soluciones Ecológicas for supplying the sorbents.

Funding

This work was supported by the financial support of the Santander-UCM 2018 project (PR108/20-07) and by the contracts of research assistant from the Community of Madrid through the program “Garantía Juvenil” [PEJ-2020-AI/IND-17675 and PEJ-2020-AI/IND-18116].

References

[1] Brutland, Report of the World Commission on Environment and Development, (1987). https://digitallibrary.un.org/record/139811 (accessed April 10, 2022).
[2] A. Endo, I. Tsurita, K. Burnett, P.M. Orencio, A review of the current state of research on the water, energy, and food nexus, J. Hydrol. Reg. Stud. 11 (2017) 20–30, https://doi.org/10.1016/j.ejrh.2015.11.010.
[3] R.S. Ramalho, Tratamiento de aguas residuales, Reverte, 2021.
[4] M.& Eddy, Ingeniería de aguas residuales, McGraw-Hill, 2001.
[5] L. Tirado Amador, F. Martínez, L. Hernández, L. Vergara, J. Suárez, Niveles de metales pesados en muestras biológicas y su importancia en salud, Rev. Nac. Odontol. 11 (2015), https://doi.org/10.16925/od.v11i21.895.
[6] M.A. Barakat, New trends in removing heavy metals from industrial wastewater, Arab. J. Chem. 4 (2011) 361–377, https://doi.org/10.1016/j.arabjc.2010.07.019.
[7] G. Blengini, C. Latunussa, U. Eynard, C. Matos, K. Georgitzikis, C. Pavel, S. Carrara, L. Mancini, M. Unguru, D. Blagoeva, F. Mathieux, D. Pennington, Study on the EU’s list of Critical Raw Materials (2020) Final Report, 2020. https://doi.org/10.2873/11619.
[8] H. Wang, K. Huang, Y. Zhang, X. Chen, W. Jin, S. Zheng, Y. Zhang, P. Li, Recovery of Lithium, Nickel, and Cobalt from Spent Lithium-Ion Battery Powders by Selective Ammonia Leaching and an Adsorption Separation System, ACS Sustain. Chem. Eng. 5 (2017) 11489–11495, https://doi.org/10.1021/acssuschemeng.7b02700.
[9] S. Rahimifard, H. Trollman, UN Sustainable Development Goals: an engineering perspective, Int. J. Sustain. Eng. 11 (2018) 1–3, https://doi.org/10.1080/19397038.2018.1434985.
[10] D.L. Thompson, J.M. Hartley, S.M. Lambert, M. Shiref, G.D.J. Harper, E. Kendrick, P. Anderson, K.S. Ryder, L. Gaines, A.P. Abbott, The importance of design in lithium ion battery recycling – a critical review, Green Chem. 22 (2020) 7585–7603, https://doi.org/10.1039/D0GC02745F.
[11] K.C. Michaels, The Role of Critical Minerals in Clean Energy Transitions, in: 2021: p. 7.
[12] A.D. Patricia, B. Darina, P. Claudiu, A. Nikolaos, Cobalt: demand-supply balances in the transition to electric mobility, in: 2018. https://doi.org/10.2760/97710.
[13] C. Peng, J. Hamuyuni, B.P. Wilson, M. Lundström, Selective reductive leaching of cobalt and lithium from industrially crushed waste Li-ion batteries in sulfuric acid system, Waste Manag. 76 (2018) 582–590, https://doi.org/10.1016/j.wasman.2018.02.052.
[14] A. Azimi, A. Azari, M. Rezakazemi, M. Ansarpour, Removal of Heavy Metals from Industrial Wastewaters: A Review, 4 (2017) 37–59. https://doi.org/10.1002/cben.201600010.

[15] S.E. Bailey, T.J. Olin, R.M. Bricka, D.D. Adrian, A review of potentially low-cost sorbents for heavy metals, Water Res. 33 (1999) 2469–2479, https://doi.org/10.1016/S0043-1354(98)00475-8.

[16] S. Mona, S.E. Gasser, J.A.D. Rizk, Adsorption and pre-concentration of Co(II) from aqueous solution using a heteropoly acid prepared sorbent, Part. Sci. Technol. 38 (2020) 166–175, https://doi.org/10.1080/02726351.2018.1518941.

[17] P. Zhang, T. Yokoyama, O. Itabashi, Y. Wakui, T.M. Suzuki, K. Inoue, Recovery of metal values from spent nickel–metal hydride rechargeable batteries, J. Power Sources. 77 (1999) 116–122, https://doi.org/10.1016/S0378-7753(98)00182-7.

[18] E. Worch, Adsorption Technology in Water Treatment: Fundamentals, Processes, and Modeling, Walter de Gruyter, 2012.

[19] M.M. Hassanien, W.I. Mortada, I.M. Kenawy, H. El-Daly, Solid Phase Extraction and Preconcentration of Trace Gallium, Indium, and Thallium Using New Modified Amino Silica, Appl. Spectrosc. 71 (2017) 288–299, https://doi.org/10.1177/0003702816654166.

[20] A.C. Sonoc, J. Jeswiet, N. Murayama, J. Shibata, A study of the application of Donnan dialysis to the recycling of lithium ion batteries, Hydrometallurgy 175 (2018) 133–143, https://doi.org/10.1016/j.hydromet.2017.10.004.

[21] F. Cecen, Ö. Aktaş, Activated Carbon for Water and Wastewater Treatment: Integration of Adsorption and Biological Treatment, 388 pages, ISBN: 978-3-527-32471-2, Wiley-VCH, 2011.

[22] T.M. Budnyak, J. Piątek, I.V. Pylypchuk, M. Klimpel, O. Sevastyanova, M. E. Lindström, V.M. Gun'ko, A. Slabon, Membrane-Filtered Kraft Lignin-Silica Hybrids as Bio-Based Sorbents for Cobalt(II) Ion Recycling, ACS, Omega. 5 (19) (2020) 10847–10856.

[23] J. Piątek, S. Afyon, T.M. Budnyak, S. Budnyk, M.H. Sipponen, A. Slabon, Sustainable Li-Ion Batteries: Chemistry and Recycling, Adv. Energy Mater. 11 (2021) 2003456, https://doi.org/10.1002/aenm.202003456.

[24] E. Asadi Dalini, G.h. Karimi, S. Zandevakili, Treatment of valuable metals from leaching solution of spent lithium-ion batteries, Miner. Eng. 173 (2021), 107226, https://doi.org/10.1016/j.mineng.2021.107226.

[25] K. Kim, D. Raymond, R. Candeago, X. Su, Selective cobalt and nickel electrodeposition for lithium-ion battery recycling through integrated electrolyte and interface control, Nat. Commun. 12 (2021) 6554, https://doi.org/10.1038/s41467-021-26814-7.

[26] M.A. Islam, D.W. Morton, B.B. Johnson, B.K. Pramanik, B. Mainali, M.J. Angove, Opportunities and constraints of using the innovative adsorbents for the removal of cobalt(II) from wastewater: A review, Environ. Nanotechnol. Monit. Manag. 10 (2018) 435–456, https://doi.org/10.1016/j.enmm.2018.10.003.

[27] A. Rodríguez, J. Gómez, Chapter 6: Basicity in zeolites, New Top. Catal. Res. 2006 (2006) 197–220.

[28] G. Zhao, J. Li, X. Ren, C. Chen, X. Wang, Few-layered graphene oxide nanosheets as superior sorbents for heavy metal ion pollution management, Environ. Sci. Technol. 45 (2011) 10454–10462, https://doi.org/10.1021/es203439v.

[29] S. De Gisi, G. Lofrano, M. Grassi, M. Notarnicola, Characteristics and adsorption capacities of low-cost sorbents for wastewater treatment: A review, Sustain. Mater. Technol. 9 (2016) 10–40, https://doi.org/10.1016/j.susmat.2016.06.002.

[30] S. Babel, T.A. Kurniawan, Low-cost adsorbents for heavy metals uptake from contaminated water: a review, J. Hazard. Mater. 97 (2003) 219–243, https://doi.org/10.1016/S0304-3894(02)00263-7.

[31] O.E. Abdel Salam, N.A. Reiad, M.M. ElShafei, A study of the removal characteristics of heavy metals from wastewater by low-cost adsorbents, J. Adv. Res. 2 (2011) 297–303, https://doi.org/10.1016/j.jare.2011.01.008.

[32] A. Ghaemi, M. Torab-Mostaedi, M. Ghannadi-Maragheh, Characterizations of Strontium(II) and Barium(II) Adsorption from Aqueous Solutions Using Dolomite Powder, J. Hazard. Mater. 190 (2011) 916–921, https://doi.org/10.1016/j.jhazmat.2011.04.006.

[33] M. Mohammadi, A. Ghaemi, M. Torab-Mostaedi, M. Asadollahzadeh, A. Hemmati, Adsorption of cadmium (II) and nickel (II) on dolomite powder, Desalination, Water Treat. 53 (2015) 149–157, https://doi.org/10.1080/19443994.2013.836990.

[34] E. Stefaniak, R. Dobrowolski, P. Staszczuk, On the Adsorption of Chromium(VI) Ions on Dolomite and 'Dolomitic Sorbents', Adsorpt. Sci. Technol. 18 (2000) 107–115, https://doi.org/10.1260/0263617001493323.

[35] A.I. Ivanets, N.V. Kitikova, I.L. Shashkova, O.V. Oleksiienko, I. Levchuk, M. Sillanpää, Removal of Zn2+, Fe2+, Cu2+, Pb2+, Cd2+, Ni2+ and Co2+ ions from aqueous solutions using modified phosphate dolomite, J. Environ. Chem. Eng. 2 (2014) 981–987, https://doi.org/10.1016/j.jece.2014.03.018.

[36] E.E. ElSayed, Natural diatomite as an effective adsorbent for heavy metals in water and wastewater treatment (a batch study), Water Sci. 32 (2018) 32–43, https://doi.org/10.1016/j.wsj.2018.02.001.

[37] J.N. Bracco, S.S. Lee, J.E. Stubbs, P.J. Eng, S. Jindra, D.M. Warren, A. Kommu, P. Fenter, J.D. Kubicki, A.G. Stack, Simultaneous Adsorption and Incorporation of Sr2+ at the Barite (001)–Water Interface, J. Phys. Chem. C 123 (2019) 1194–1207, https://doi.org/10.1021/acs.jpcc.8b08848.

[38] N. Gupta, Adsorption Of Cobalt(II) From Aqueous Solution Onto Hydroxyapatite/Zeolite Composite, Adv. Mater. Lett. 2 (4) (2011) 309–312.

[39] A. Rodríguez, P. Sáez, E. Díez, J.M. Gómez, J. García, I. Bernabé Vírseda, Highly efficient low-cost zeolite for cobalt removal from aqueous solutions: Characterization and performance, Environ. Prog. Sustain. Energy 38 (s1) (2019) S352–S365, https://doi.org/10.1002/ep.13057.

[40] J.-M. Park, S.-K. Kam, M.-G. Lee, Adsorption Characteristics of Lithium Ion by Zeolite Modified in K^+, Na^+, Mg^{2+}, Ca^{2+}, and Al^{3+} Forms, J. Environ. Sci. Int. 22 (12) (2013) 1651–1660, https://doi.org/10.5322/JESI.2013.22.12.1651.

[41] M.N. Siddiqui, B. Chanbasha, A.A. Al-Arfaj, T. Kon'kova, I. Ali, Super-fast removal of cobalt metal ions in water using inexpensive mesoporous carbon obtained from industrial waste material, Environ. Technol. Innov. 21 (2021) 101257, https://doi.org/10.1016/j.eti.2020.101257.

[42] H. Farzaneh, J. Saththasivam, G. McKay, P. Parthasarathy, Adsorbent Minimization for Removal of Ibuprofen from Water in a Two-Stage Batch Process, Processes. 10 (2022) 453, https://doi.org/10.3390/pr10030453.

[43] A.B. de Haan, Adsorption and ion exchange, in: Chapter 9 Adsorpt. Ion Exch., De Gruyter, 2015: pp. 177–196. https://www.degruyter.com/document/doi/10.1515/9783110336726-010/pdf (accessed July 8, 2022).

[44] J.M. Gómez, E. Díez, A. Rodríguez, C. Jiménez, Deoxygenation of methyl laurate: influence of cation and mesoporosity in fau zeolites, J. Porous Mater. 28 (5) (2021) 1355–1360, https://doi.org/10.1007/s10934-021-01086-0.

[45] J. Galán, A. Rodríguez, J.M. Gómez, S.J. Allen, G.M. Walker, Reactive dye adsorption onto a novel mesoporous carbon, Chem. Eng. J. 219 (2013) 62–68, https://doi.org/10.1016/j.cej.2012.12.073.

[46] G.-B. Cai, S.-F. Chen, L. Liu, J. Jiang, H.-B. Yao, A.-W. Xu, S.-H. Yu, 1,3-Diamino-2-hydroxypropane-N,N,N′,N′-tetraacetic acid stabilized amorphous calcium carbonate: Nucleation, transformation and crystal growth, CrystEngComm 12 (1) (2010) 234–241, https://doi.org/10.1039/b911426m.

[47] H. Hadoun, Z. Sadaoui, N. Souami, D. Sahel, I. Toumert, Characterization of mesoporous carbon prepared from date stems by H3PO4 chemical activation, Appl. Surf. Sci. 280 (2013) 1–7, https://doi.org/10.1016/j.apsusc.2013.04.054.

[48] A. Micheal, P. Muyoma, Characterization of Chemically Activated Carbons Produced from Coconut and Palm Kernel Shells Using SEM and FTIR Analyses, 9 (2021) 90–96. https://doi.org/10.11648/j.ajac.20210903.15.

[49] M. Walczyk, A. Świątkowski, M. Pakula, S. Biniak, Electrochemical studies of the interaction between a modified activated carbon surface and heavy metal ions, J. Appl. Electrochem. 35 (2005) 123–130, https://doi.org/10.1007/s10800-004-2399-0.

[50] Z. Wu, P.A. Webley, D. Zhao, Comprehensive study of pore evolution, mesostructural stability, and simultaneous surface functionalization of ordered mesoporous carbon (FDU-15) by wet oxidation as a promising adsorbent, Langmuir ACS J. Surf. Colloids. 26 (2010) 10277–10286, https://doi.org/10.1021/la100455w.

[51] J.M. Gómez, E. Díez, I. Bernabé, P. Sáez, A. Rodríguez, Effective Adsorptive Removal of Cobalt Using Mesoporous Carbons Synthesized by Silica Gel Replica Method, Environ. Process. 5 (2018) 225–242, https://doi.org/10.1007/s40710-018-0304-9.

[52] P. Moulin, H. Roques, Zeta potential measurement of calcium carbonate, J. Colloid Interface Sci. 261 (2003) 115–126, https://doi.org/10.1016/S0021-9797(03)00057-2.

[53] A. Krishnan, T. Anirudhan, Kinetic and equilibrium modelling of cobalt(II) adsorption onto bagasse pith based sulphurised activated carbon, Chem. Eng. J. 137 (2008) 257–264, https://doi.org/10.1016/j.cej.2007.04.029.

[54] W. Zyzak, F. Brzóska, B. Brzóska, J. Michalec-Dobija, The solubility and availability of magnesium from calcium-magnesium carbonate and magnesium carbonate, J. Anim. Feed Sci. 11 (2002) 695–707, https://doi.org/10.22358/jafs/67927/2002.

[55] L. Sherman, P. Barak, Solubility and Dissolution Kinetics of Dolomite in Ca–Mg–HCO/CO Solutions at 25°C and 0.1 MPa Carbon Dioxide, Soil Sci. Soc. Am. J. - SSSAJ. 64 (2000), https://doi.org/10.2136/sssaj2000.6461959x.

[56] G.H. Nancollas, N. Purdie, Crystallization of barium sulphate in aqueous solution, Trans. Faraday Soc. 59 (1963) 735–740, https://doi.org/10.1039/TF9635900735.

[57] A.B. Cummins, L.B. Miller, Diatomaceous Earth - Equilibrium and Rate of Reaction in the System Hydrated Lime-Diatomaceous Silica-Water, Ind. Eng. Chem. 26 (1934) 688–693, https://doi.org/10.1021/ie50294a022.

[58] I. Barton, H. Yang, M. Barton, The mineralogy, geochemistry, and metallurgy of cobalt in the rhombohedral carbonates, Can. Mineral. 52 (2015) 653–670, https://doi.org/10.3749/canmin.1400006.

[59] E. Pehlivan, A.M. Ozkan, S. Dinç, S. Parlayici, Adsorption of Cu2+ and Pb2+ ion on dolomite powder, J. Hazard. Mater. 167 (2009) 1044–1049, https://doi.org/10.1016/j.jhazmat.2009.01.096.

[60] C. Lin, T. Kadono, K. Yoshizuka, T. Furuichi, T. Kawano, Effects of fifteen rare-earth metals on Ca2+ influx in tobacco cells, Z. Naturforschung C, J. Biosci. 61 (2006) 74–80, https://doi.org/10.1515/znc-2006-1-214.

[61] W.A. Kornicker, J.W. Morse, R.N. Damasceno, The chemistry of Co2+ interaction with calcite and aragonite surfaces, Chem. Geol. 53 (1985) 229–236, https://doi.org/10.1016/0009-2541(85)90072-5.

[62] M. Kobya, E. Demirbas, E. Senturk, M. Ince, Adsorption of heavy metal ions from aqueous solutions by activated carbon prepared from apricot stone, Bioresour. Technol. 96 (2005) 1518–1521, https://doi.org/10.1016/j.biortech.2004.12.005.

[63] S. Sato, K. Yoshihara, K. Moriyama, M. Machida, H. Tatsumoto, Influence of activated carbon surface acidity on adsorption of heavy metal ions and aromatics from aqueous solution, Appl. Surf. Sci. 253 (2007) 8554–8559, https://doi.org/10.1016/j.apsusc.2007.04.025.

[64] C.C. Pavel, D. Vuono, I.V. Asaftei, P. De Luca, N. Bilba, J.B. Nagy, A. Nastro, Study of the thermal dehydration of metal-exchange ETS-10 titanosilicate, in: J. Čejka, N. Žilková, P. Nachtigall (Eds.), Stud. Surf. Sci. Catal., Elsevier, 2005: pp. 805–812. https://doi.org/10.1016/S0167-2991(05)80416-1.

[65] E.R. Nightingale, Phenomenological Theory of Ion Solvation. Effective Radii of Hydrated Ions, J. Phys. Chem. 63 (9) (1959) 1381–1387, https://doi.org/10.1021/j150579a011.

[66] A. Füger, F. Konrad, A. Leis, M. Dietzel, V. Mavromatis, Effect of growth rate and pH on lithium incorporation in calcite, Geochim. Cosmochim. Acta 248 (2019) 14–24.

[67] R.J. Reeder, G.M. Lamble, P.A. Northrup, XAFS study of the coordination and local relaxation around Co2+, Zn2+, Pb2+, and Ba2+ trace elements in calcite, Am. Mineral. 84 (1999) 1049–1060, https://doi.org/10.2138/am-1999-7-807.
[68] Database of Zeolite Structures. HEU: Framework Type, IZA Struct. Comm. (2007). https://america.iza-structure.org/IZA-SC/framework.php?STC=HEU (accessed September 7, 2022).
[69] C.H. Giles, T.H. MacEwan, S.N. Nakhwa, D. Smith, 786. Studies in adsorption. Part XI. A system of classification of solution adsorption isotherms, and its use in diagnosis of adsorption mechanisms and in measurement of specific surface areas of solids, J. Chem. Soc. Resumed. (1960) 3973–3993, https://doi.org/10.1039/JR9600003973.